The distribution of star-forming regions in M33

Néstor Sánchez[1], Neyda Añez[2], Emilio J. Alfaro[1], and Mary Crone Odekon[3]

[1] Instituto de Astrofísica de Andalucía, CSIC, Granada, Spain
[2] Departamento de Física, Universidad del Zulia, Maracaibo, Venezuela
[3] Department of Physics, Skidmore College, Saratoga Springs, USA

Abstract

We use fractal analysis to systematically study the clustering strength of the distribution of stars, HII regions, molecular gas, and individual giant molecular clouds in M33 over a wide range of spatial scales. We find a clear transition from a scale-free behavior at small spatial scales to a nearly uniform distribution at large scales. The transition region lies in the range $\sim 500 - 1000$ pc and it separates the regime of small-scale turbulent motion from that of large-scale galactic dynamics. The three-dimensional fractal dimension of bright young stars and molecular gas at small spatial scales is $D_{f,\mathrm{3D}} \lesssim 1.9$ indicating that the interstellar medium in M33 is on average much more fragmented and irregular than the in the Milky Way.

1 Introduction

Interstellar Medium (ISM) in the Milky Way shows fractal patterns, that is, it is organized into irregular structures in a hierarchical and approximately self-similar manner in which each structure (cloud) is composed of smaller similar structures which are composed of even smaller structures and so on. This fractal structure is observed over a wide range of spatial scales from ~ 0.1 pc to ~ 100 pc or even more, and it is supposed to be a consequence of turbulent processes ocurring in the ISM [8]. The formation of stars also exhibits a spatial hierarchy ranging from the scale of a few pc for star clusters and associations up to about a kpc for so-called star complexes [7]. Fractal analysis is an appropiate tool for characterizing these hierarchical and self-similar systems. The fractal dimension D_f quantifies the degree of irregularity or clumpiness (spatial heterogeneity) of the distribution of gas or stars. The more irregular or far from homogeneity is the structure, the smaller fractal dimension values. It is often accepted that the fractal dimension of the ISM in our Galaxy has a nearly universal value [3]. From a detailed analysis of several emission maps of three different molecular clouds, [20] obtained $D_f \simeq 2.7 \pm 0.1$ with no evidence of significant variations.

An important issue is the spatial extent of this self-similar behavior. In the solar neighborhood, fractal behavior has been observed for the distribution of young open cluster and young stars at spatial scales of up to ~ 1 kpc [5]. In external galaxies, hierarchical structures extend up to $\gtrsim 1$ kpc scales for the gas and for stars and star-forming sites [2, 4]. However, there seem to be variations in the fractal properties among galaxies [17]. The distribution of gas [6], stars [13] and HII regions [17] seems to be less clustered in bright galaxies. In other words, a larger star formation rate in a galaxy tends to be correlated with a larger fractal dimension. A significant challenge in interpreting this and other results is that authors present measurements for different ranges of scales and identify their samples in different ways. Our approach in this work is to consider a case study in which we systematically analyze the clustering of different components of a single galaxy over a wide range of spatial scales. Because of its proximity, large size, and low inclination, M33 is a suitable object for this task. Thus, here we study the clustering strength in the distribution of young stars, HII regions, molecular gas, and individual giant molecular clouds (GMCs) in M33.

2   Data and method

For the distribution of stars we used the catalog of [12] to get positions and photometry of stars in M33. Stars were divided into two sets that we refer to simply as "bright" stars ($-0.3 \leq V - I \leq -0.1$ and $-6.0 \leq M_I \leq -5.0$) and "faint" stars ($-0.3 \leq V - I \leq 0.0$ and $-4.5 \leq M_I \leq -4.0$). The total numbers of stars for the bright and faint sets are 534 and 1644, respectively. For the HII regions we used the catalog of [11], from which we removed regions classified as unresolved, diffuse, linear and/or any other factor that may raise doubts on the real nature of such regions. We also removed the regions having null integrated Hα fluxes in the catalog. The total number of "bright" HII regions in M33 was 617. The distribution of 149 molecular clouds was obtained from the catalog of [16]. For the molecular gas we used high resolution CO emission data of the center region of M33 provided by Erik Rosolowsky [16]. The data cube was collapsed to produce a map of integrated intensity with a final resolution of $20''$ (93 pc). We adopted a position angle of 23 degrees and an inclination of 55 degrees to deproject the positions of stars, HII regions and GMCs. To convert angular sizes into linear sizes, we assume a distance of 960 kpc [21]. The positions of bright stars, HII regions and GMCs relative to the galactic center, and the area corresponding to the used molecular gas map are shown in Fig. 1.

The degree of clustering was measured by applying algorithms that we have previously developed and tested on simulated fractals. For the distribution of stars, HII regions and GMCs we calculated the correlation dimension D_c from the relation $C(r) \sim r^{D_c}$, where the correlation integral $C(r)$ is the average number of points within a distance r [17, 19]. In order to consider the possibility of a transition in D_c [14], we performed two separate calculations at different scales. We varied the range of spatial scales until obtaining the best result (the one with the minimum transition region that minimizes the sum of the squared residuals). For the emission map we calculated the perimeter-based dimension D_{per} from the equation $P \sim A^{D_{\mathrm{per}}/2}$ relating the perimeters P and areas A of the clouds in the map [18].
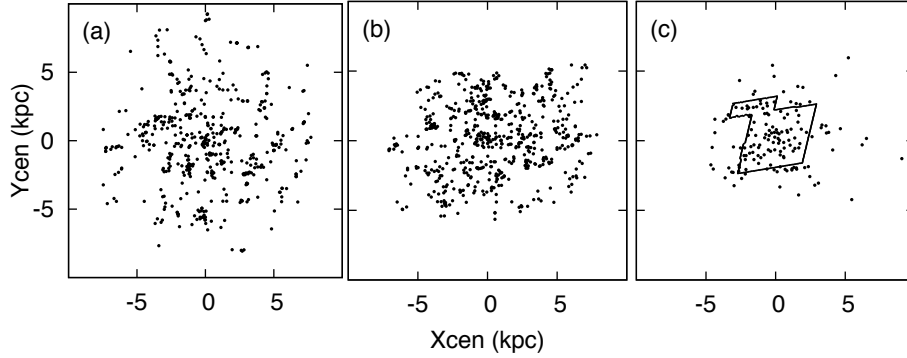
Figure 1: Spatial distributions of (a) bright stars, (b) bright HII regions and (c) GMCs in M33. The axis coordinates are positions relative to the galactic center in kpc. The inset in panel (c) shows the area corresponding to the molecular gas map.

3   Results and discussion

Figure 2 shows the correlation integral for stars, HII regions and GMCs. The slopes of the linear fits are the correlation dimensions which are shown in Table 1. This Table also shows the perimeter dimension resulting from the CO emission map. The calculated two-dimensional fractal dimensions ($D_{f,2D}$) were converted to three-dimensional dimensions ($D_{f,3D}$) using results from previous studies [18, 17]. Table 1 shows the range of $D_{f,3D}$ values that are compatible with the calculated values of $D_{f,2D}$. Several interesting conclusions can be drawn from these results, which we discuss now.

Table 1: Calculated fractal dimensions for M33

Sample	Small spatial scales[a]		Large spatial scales	
	$D_{f,2D}$[b]	$D_{f,3D}$	$D_{f,2D}$	$D_{f,3D}$
Bright stars	1.01 ± 0.05	1.0–1.9	1.93 ± 0.03	2.8–2.9
Faint stars	1.42 ± 0.04	2.2–2.4	1.89 ± 0.02	2.8–2.9
HII regions	1.48 ± 0.08	2.3–2.5	2.01 ± 0.03	2.9–3.0
Molecular clouds	$\cdots$	$\cdots$	1.98 ± 0.04	2.8–3.0
CO emission map	1.65 ± 0.06	1.6–1.8	$\cdots$	$\cdots$

[a]For stars and HII regions small spatial scale means $\lesssim$ 500 pc and large scale means $\gtrsim$ 1 kpc. For molecular gas large scale is $\gtrsim$ 500 pc (distribution of clouds) and small scale is $\lesssim$ 500 pc (CO map).
[b]$D_{f,2D}$ refers either to the two-dimensional correlation dimension D_c (for the distribution of stars, HII regions and GMCs) or to the perimeter-area based dimension D_{per} (for the CO map). $D_{f,3D}$ is the corresponding three-dimensional fractal dimension.
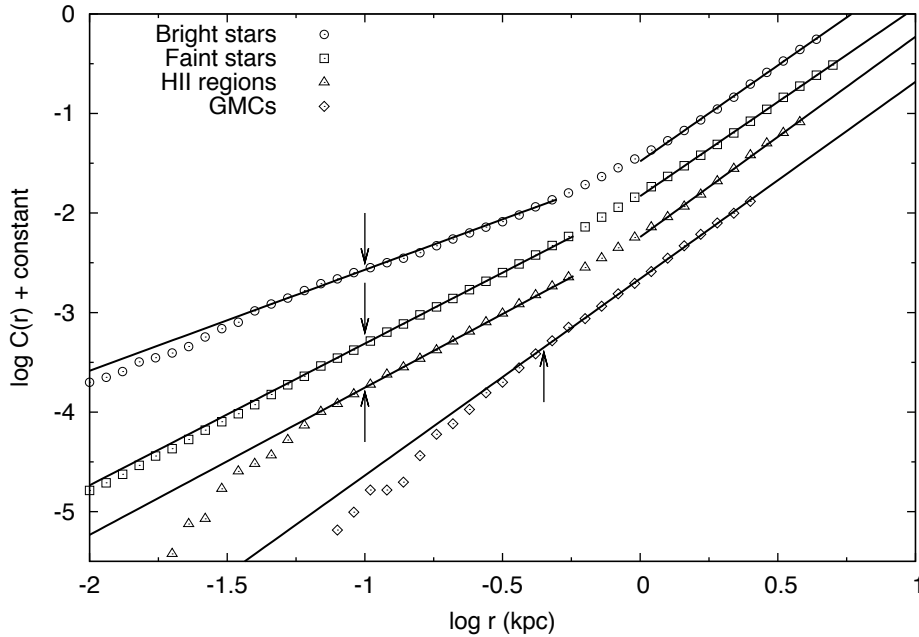
Figure 2: Correlation integral $C(r)$ for the samples of bright stars (circles), faint stars (squares), HII regions (triangles) and GMCs (rhombuses). The data have been arbitrarily shifted downward (except the top one) for clarity. Vertical arrows indicate the points above which the algorithm gives reliable values of $C(r)$ and performs the linear fits (solid lines). Different fits were done below and above the range without any straight line, except for the GMCs that do not show any change in the slope.

3.1 Transition region

All of the objects except the GMCs exhibit scale-free clustering on small scales and a clear transition to a higher slope at larger spatial scales (Fig. 2). At small scales the correlation dimension of the distribution of stars and HII regions is $\lesssim 1.5$ whereas at large scales it is $\gtrsim 1.9$, and the differences are always larger than the associated uncertainties (Table 1). The spatial scale where this transition takes place is roughly the same for each component ($\sim 500 - 1000$ pc). A transition from a smaller correlation dimension to a larger one was reported by [14] for young stars in M33. However, [1] did not find any characteristic size for the distribution of star-forming regions. Here we provide a detailed quantification of this transition and observe it for the first time for the distribution of HII regions. The transition is not observed for the distribution of GMCs but, given the limited number of data points for this sample ($N = 149$), the lower limit of reliable values is higher than for the other objects ($r \gtrsim 500$ pc).

What is the nature of this transition? [15] argued that there must be a physical transition in the statistical properties of the flow close to the disk scale height. In turbulent flows the energy is injected at certain spatial scale and then it "cascades" to smaller scales.

But there are many possible energy sources that may be relevant at different levels. A possible consequence of this may be different distribution patterns at different size ranges. Even though the underlying turbulent structure tends to be the same, non-turbulent motions acting on galactic scales could modify the final structure at those scales. In other words, the power law behavior at small spatial scales would be a direct consequence of the self-similar turbulent motions in the medium, but this turbulence is unlikely to extend to very large scales, where two-dimensional flows should dominate the dynamics. Thus, we identify a characteristic spatial scale (around $500 - 1000$ pc) that separates the regime where coherent star formation is occurring in a turbulent medium from the regime that is organized by large-scale galactic dynamics. Interestingly, the behavior we observe is that all the fractal dimensions at $r \gtrsim 1$ kpc are within a narrow range of values ($D_{f,2D} = 1.9 - 2.0$, or $D_{f,3D} = 2.8 - 3.0$) that are consistent with essentially uniform (random) distributions.

3.2   Evolutionary effects

Young, newborn stars should reflect the same conditions of the ISM from which they were formed. Therefore, it is reasonable to assume that the fractal dimension of the distribution of new-born stars should be nearly the same as that of the molecular gas from which they are formed. Our results are roughly consistent with this idea within the rather large uncertainties for $D_{f,3D}$. Both bright stars and molecular gas are distributed with $D_{f,3D} \lesssim 1.9$. However, faint stars and HII regions have significantly higher fractal dimensions. We interpret these higher dimensions in terms of evolutionary effects. It seems that the initial clumpy distribution of star-forming sites may evolve towards a smoother distribution. This effect has been observed for the distributions of young stars in LMC [2] and SMC [10] and for the stars clusters in both galaxies [4]. It has been shown that the brightest HII regions in spiral galaxies (which reflect, in a first approximation, the initial distribution of star-forming sites) tend to be distributed in more clumpy patterns than the low-brightness regions [17]. A smoother distribution means a higher fractal dimension, and this is what we found for faint stars and HII regions at small scales for which $D_{f,3D} \simeq 2.2 - 2.5$.

3.3   Fractal structure in M33

The three-dimensional fractal dimension of the distribution of molecular gas in M33 is $D_{f,3D} \simeq 1.6 - 1.8$. It is a very interesting to note that this value is much smaller than the fractal dimension of molecular clouds in the Milky Way, which is in the range $D_{f,3D} \simeq 2.6 - 2.8$ [18, 20]. That is, molecular clouds in M33 exhibit a much more fragmented and irregular structure than in the Milky Way. This result may yield some clues about the main physical processes that determine the structure of the ISM. In principle, if the main physical mechanisms acting were not the same we would expect different global properties for the ISM. Simulations of turbulent fluids produce very different structures depending on which processes are considered in the system. For example, [9] showed that simulations of supersonic isothermal turbulence in the extreme case of purely compressive energy injection, produce a significantly smaller fractal dimension for the density distribution ($D_f \sim 2.3$) than in the case of purely solenoidal forcing ($D_f \sim 2.6$). Although it is widely accepted that turbulence is the primary driver of

the structure and motion of the ISM, the main energy sources for this turbulence are not yet well established. Obviously, more detailed studies are needed to clarify this point but in this work we have found a significant and remarkable difference in the internal structure of GMCs between M33 and the Milky Way.

Acknowledgments

References

[1] Bastian, N., Ercolano, B., Gieles, M., Rosolowsky, E., Scheepmaker, R. A., Gutermuth, R., & Efremov, Y. 2007, MNRAS, 379, 1302

[2] Bastian, N., Gieles, M., Ercolano, B., & Gutermuth, R. 2009, MNRAS, 392, 868

[3] Bergin, E. A., & Tafalla, M. 2007, ARA&A, 45, 339

[4] Bonatto, C., & Bica, E. 2010, MNRAS, 403, 996

[5] de la Fuente Marcos, R., & de la Fuente Marcos, C. 2009, ApJ, 700, 436

[6] Dutta, P., Begum, A., Bharadwaj, S., & Chengalur, J. N. 2009, MNRAS, 398, 887

[7] Efremov, Y. N. 1995, AJ, 110, 2757

[8] Elmegreen, B. G., & Scalo, J. 2004, ARA&A, 42, 211

[9] Federrath, C., Klessen, R. S., & Schmidt, W. 2009, ApJ, 692, 364

[10] Gieles, M., Bastian, N., & Ercolano, B. 2008, MNRAS, , 391, L93

[11] Hodge, P. W., Balsley, J., Wyder, T. K., & Skelton, B. P. 1999, PASP, 111, 685

[12] Massey, P., Olsen, K. A. G., Hodge, P. W., Strong, S. B., Jacoby, G. H., Schlingman, W., & Smith, R. C. 2006, AJ, 131, 2478

[13] Odekon, M. C. 2006, AJ, 132, 1834

[14] Odekon, M. C. 2008, ApJ, 681, 1248

[15] Padoan, P., Kim, S., Goodman, A., & Staveley-Smith, L. 2001, ApJ, 555, L33

[16] Rosolowsky, E., Keto, E., Matsushita, S., & Willner, S. P. 2007, ApJ, 661, 830

[17] Sánchez, N., & Alfaro, E. J. 2008, ApJS, 178, 1

[18] Sánchez, N., Alfaro, E. J., & Pérez, E. 2005, ApJ, 625, 849

[19] Sánchez, N., Alfaro, E. J., Elias, F., Delgado, A. J., & Cabrera-Caño, J. 2007a, ApJ, 667, 213

[20] Sánchez, N., Alfaro, E. J., & Pérez, E. 2007b, ApJ, 656, 222

[21] Urbaneja, M. A., Kudritzki, R.-P., Jacobs, B. A., Bresolin, F., & Przybilla, N. 2009, ApJ, 704, 1120